Gulf Journal of Mathematics
Vol 24, Issue 2 (2026) 1-10

ISSN: 2309-4966
https://doi.org/10.56947/hvhm3402

OPTIMAL CONTROL OF EXTREME EPIDEMIC RISKS

KPÈBBÈWÈRÈ CÉDRIC SOME[1], BIRBA MAMADOU[2*] and VINI YVES BERNADIN LOYARA[3]

Abstract. We propose a stochastic framework for the optimal control of epidemics, combining an SIR model with Conditional Value-at-Risk. The dependence between transmission and recovery rates is modeled using four copulas: Gaussian, Student, Archimax, and Vine. We establish theoretical results on existence, uniqueness, stability, and robustness of the optimal control. Simulations on COVID-19 data from Burkina Faso show that Archimax reduces the risk measure by 31% compared to the Gaussian copula. A complementary Hidden Markov analysis identifies three epidemic regimes with strong persistence, highlighting the value of modeling tail dependence for epidemic risk management.

Keywords. Optimal control, risk measures, copulas, Markov chains, SIR model, COVID-19
2020 Mathematics Subject Classification. Primary 49J15, 49K15; Secondary 62H05, 93C95, 93D20, 60J10

1. Introduction

The COVID-19 pandemic demonstrated the importance of mathematical models for public health decision-making, particularly in resource-limited countries such as Burkina Faso. Compartmental models coupled with optimal control have been widely used to design containment and vaccination strategies [14, 12]. Most existing approaches, however, minimize the expected number of cases, thereby neglecting the worst-case scenarios that are the primary concern of decision-makers.

In finance, such concerns are addressed by coherent risk measures, notably Value-at-Risk and Conditional Value-at-Risk [1, 13]. These measures quantify the average loss in the worst cases and possess convexity properties suitable for optimization. Moreover, classical epidemiological models often assume independence between the transmission rate and the recovery rate, an unrealistic hypothesis. Copulas provide a flexible framework for modeling nonlinear dependencies,

Date: Received: Aug 24, 2026; Revised: Sep 21, 2026; Accepted: Sep 28, 2026.
* Corresponding author
© The Author(s) 2026. This article is licensed under a Creative Commons Attribution-NonCommercial-NoDerivatives 4.0 International License. To view a copy of the licence, visit https://creativecommons.org/licenses/by-nc-nd/4.0/.

including tail dependence [11]. Recent methodological advances in copula estimation and testing, such as those proposed by [3] and [2] in this journal, are directly relevant to our framework.

The objective of this article is to merge epidemiological modeling, optimal control, and risk management into a unified framework. We use four copula families: Gaussian, Student, Archimax, and Vine. We also apply a Hidden Markov Model as a complementary diagnostic tool for regime detection.

The article is organized as follows. Section 2 presents the mathematical preliminaries. Section 3 formulates the optimal control problem. Section 4 establishes the theoretical results. Section 5 describes the numerical methodology. Section 6 reports the simulations and results. Section 7 concludes. Appendix A contains the complementary Hidden Markov analysis.

2. Mathematical preliminaries

We consider the standard SIR model with control $u(t) \in [0, u_{\max}]$:

$$\begin{cases} \dot{S} = -\beta SI + \nu R, \\ \dot{I} = \beta SI - \gamma I - uI, \\ \dot{R} = \gamma I + uI - \nu R, \end{cases} \tag{2.1}$$

with initial conditions $S(0) = S_0 > 0$, $I(0) = I_0 > 0$, and $R(0) = R_0 \geq 0$. The parameters β and γ denote the transmission and recovery rates, and ν the immunity loss rate. This model is classical; a detailed derivation can be found in [12].

The dependence between β and γ is modeled by a copula C_θ satisfying

$$F_{(\beta,\gamma)}(b, g) = C_\theta\big(F_\beta(b), F_\gamma(g)\big), \tag{2.2}$$

where F_β and F_γ are the marginal distribution functions. We consider four families. The Gaussian copula is $C_{\text{Gauss}}(u, v; \rho) = \Phi_\rho(\Phi^{-1}(u), \Phi^{-1}(v))$ with $\rho \in (-1, 1)$ and no tail dependence. The Student copula is $C_{\nu,\rho}(u, v) = t_{\nu,\rho}(t_\nu^{-1}(u), t_\nu^{-1}(v))$ with lower tail dependence coefficient $\lambda_L = 2t_{\nu+1}(-\sqrt{(\nu+1)(1-\rho)/(1+\rho)})$. The Archimax copula is $C_{\text{Archimax}}(u, v; \theta, \psi) = \psi^{-1}\big((\psi(u)+\psi(v))A(\psi(u)/(\psi(u)+\psi(v)))\big)$, which combines global dependence and extreme tails. The Vine copula is constructed as a decomposition into pairs of conditional copulas; a detailed account is given in [4].

Let X be a loss variable. The Value-at-Risk at level $\alpha \in (0, 1)$ is $\text{VaR}_\alpha(X) = \inf\{x : \mathbb{P}(X \leq x) \geq \alpha\}$. The Conditional Value-at-Risk is $\text{CVaR}_\alpha(X) = \mathbb{E}[X \mid X \geq \text{VaR}_\alpha(X)]$ for continuous distributions. In general, the Rockafellar–Uryasev representation $\text{CVaR}_\alpha(X) = \min_{z\in\mathbb{R}}\{z + (1-\alpha)^{-1}\mathbb{E}[(X - z)_+]\}$ holds [13]. The Tail Value-at-Risk is $\text{TVaR}_\alpha(X) = (1-\alpha)^{-1}\mathbb{E}[X \cdot \mathbf{1}_{\{X \geq \text{VaR}_\alpha(X)\}}]$, which coincides with the CVaR for continuous distributions. The Extreme Tail Value-at-Risk at a higher level $\beta > \alpha$ is $\text{XTVaR}_{\alpha,\beta}(X) = \mathbb{E}[X \mid X \geq \text{VaR}_\beta(X)]$.

3. Problem formulation

We consider the classical cost functional

$$J(u) = \mathbb{E}\left[I(T) + \int_0^T \frac{p}{2}u^2(t)\,dt\right], \tag{3.1}$$

where $p > 0$ is the unit cost of containment. We replace the expectation by the CVaR and consider the problem

$$\min_{u\in\mathcal{U}}\left\{\mathrm{CVaR}_\alpha(I(T)) + \int_0^T \frac{p}{2}u^2(t)\,dt\right\}, \tag{3.2}$$

where $\mathcal{U} = \{u : [0,T] \to [0, u_{\max}],\ \text{measurable}\}$. This formulation penalizes both extreme losses and the intensity of containment.

4. Theoretical results

The first result concerns the regularity of the map $u \mapsto I(T)$.

Lemma 4.1. *The solution $I(T)$ of (2.1) depends continuously on $u \in L^2([0,T])$, and the map $u \mapsto \mathrm{CVaR}_\alpha(I(T))$ is convex.*

Proof. The SIR system has a Lipschitz continuous right-hand side in (S, I, R) for bounded u. By Grönwall's inequality, the solution operator is continuous with respect to the control. The CVaR is convex as a function of the random variable $I(T)$ [13], and composition with a continuous linear operator preserves convexity. □

Theorem 4.2. *Under the assumptions that the marginals of β and γ are square-integrable on $[0,T]$, that the copula C_θ is continuous with continuous density c_θ, and that $p > 0$ and $u_{\max} < \infty$, the problem (3.2) admits a unique optimal solution $u^* \in \mathcal{U}$. This solution is characterized by the Pontryagin Minimum Principle with terminal condition*

$$\lambda_I(T) = -\frac{1}{1-\alpha}\mathbf{1}_{\{I(T)\geq \mathrm{VaR}_\alpha(I(T))\}}. \tag{4.1}$$

Proof. The set $\mathcal{U}$ is closed, bounded, and convex in $L^2([0,T])$, hence weakly compact. By the preceding lemma, the map $u \mapsto \mathrm{CVaR}_\alpha(I(T))$ is continuous and convex, and the quadratic term $(p/2)\int u^2$ is weakly lower semi-continuous. By the Weierstrass theorem for weakly lower semi-continuous functionals, a minimizer exists. Uniqueness follows from the strict convexity of the quadratic term. The terminal condition is obtained by differentiating the terminal cost $\mathrm{CVaR}_\alpha(I(T))$ with respect to $I(T)$; the subgradient is $(1-\alpha)^{-1}\mathbf{1}_{\{I(T)\geq \mathrm{VaR}_\alpha(I(T))\}}$, and the negative sign follows from the PMP convention. □

We now complete the SIR model with a population dynamics $\dot{N}(t) = \Lambda - \mu N(t) - \mu_c I(t)$, where $N = S + I + R$, $\Lambda > 0$, $\mu > 0$, and $\mu_c > 0$. The augmented system is

$$\begin{cases} \dot{S} = -\beta SI + \nu R + \Lambda - \mu S, \\ \dot{I} = \beta SI - \gamma I - uI - \mu_c I, \\ \dot{R} = \gamma I + uI - \nu R - \mu R, \end{cases} \tag{4.2}$$

and the infection-free equilibrium is $(S^*, 0, 0)$ with $S^* = \Lambda/\mu$.

Theorem 4.3. *Assume that $\beta(t)$ and $\gamma(t)$ are bounded with $0 < \beta_{\min} \leq \beta(t) \leq \beta_{\max}$ and $0 < \gamma_{\min} \leq \gamma(t) \leq \gamma_{\max}$, that $p > (\lambda_I - \lambda_R)I_{\max}/\epsilon$ for some $\epsilon > 0$, and that $\mu_c > 0$. Let $u^*(t) = \min(u_{\max}, \max(0, (\lambda_I(t) - \lambda_R(t))I(t)/p))$. Then there exists $\delta > 0$ such that the Lyapunov function $V = \frac{1}{2}(S - S^*)^2 + \frac{1}{2}I^2 + \frac{1}{2}R^2$ satisfies $\dot{V} \leq -\delta V$, which implies exponential stability of the closed-loop system around $(S^*, 0, 0)$.*

Proof. Using $\Lambda - \mu S = -\mu(S - S^*)$ and Young's inequality $2|ab| \leq \eta a^2 + \eta^{-1}b^2$, we bound the cross terms in $\dot{V}$. Choosing the constants $\eta_1 = \mu/(\beta_{\max} S_{\max})$ and $\eta_2 = \mu/(\gamma_{\max} + u_{\max})$ yields a quadratic form in $(S - S^*)$, I, and R whose coefficients are all strictly negative under the stated hypotheses. The existence of $\delta > 0$ follows. □

Lemma 4.4. *For a fixed control u, the map $\chi_U \mapsto \mathrm{CVaR}_\alpha(I_u(T))$ is strictly increasing, where χ_U denotes the upper tail dependence coefficient of the copula governing (β, γ).*

Proof. Let C_1 and C_2 be two copulas with upper tail dependence coefficients $\chi_U^{(1)} > \chi_U^{(2)}$. The distribution of $I(T)$ under C_1 has heavier right tails than under C_2, because a larger χ_U implies a larger probability of simultaneous extreme realizations of β and γ. Since the CVaR increases with first-order stochastic dominance of the right tail, the conclusion follows. □

Theorem 4.5. *Let C_1 denote the Archimax copula, C_2 the Gaussian, C_3 the Student, and C_4 the Vine copula, with corresponding optimal controls u_i^*. Then for any $\alpha \in (0, 1)$,*

$$\mathrm{CVaR}_\alpha(I_{u_1^*}(T)) \leq \mathrm{CVaR}_\alpha(I_{u_i^*}(T)), \quad i = 2, 3, 4. \tag{4.3}$$

Moreover, the average control intensities satisfy $\bar{u}_1 \geq \bar{u}_i$ for $i = 2, 3, 4$.

Proof. The upper tail dependence coefficient of a copula C is

$$\chi_U(C) = \lim_{q \to 1^-} \mathbb{P}(U > q \mid V > q) = \lim_{q \to 1^-} \frac{1 - 2q + C(q, q)}{1 - q}.$$

For the Gaussian copula, $\chi_U(C_2) = 0$. For the Student copula with $\nu \approx 16$, we have $\chi_U(C_3) \approx 0.28$. For the Archimax copula with a Gumbel generator and $\theta \approx 1.5$, we have $\chi_U(C_1) \approx 0.39$. For the Vine copula, $\chi_U(C_4) \in [0.15, 0.25]$. By the preceding lemma, $\mathrm{CVaR}_\alpha(I(T))$ is strictly increasing in χ_U, so the Archimax copula imposes the strictest control, and consequently yields the smallest CVaR. □

5. Numerical methodology

The Hamiltonian associated with (3.2) is

$$H = \lambda_S(-\beta SI + \nu R) + \lambda_I(\beta SI - \gamma I - uI) + \lambda_R(\gamma I + uI - \nu R) + \frac{p}{2}u^2. \tag{5.1}$$

The adjoint equations are

$$\begin{cases} \dot{\lambda}_S = \lambda_S \beta I - \lambda_I \beta I, \\ \dot{\lambda}_I = \lambda_S \beta S - \lambda_I(\beta S - \gamma - u) - \lambda_R(\gamma + u), \\ \dot{\lambda}_R = -\lambda_S \nu + \lambda_R \nu, \end{cases} \tag{5.2}$$

and the optimality condition gives

$$u^*(t) = \min\left(u_{\max}, \max\left(0, \frac{(\lambda_I(t) - \lambda_R(t))I(t)}{p}\right)\right). \tag{5.3}$$

We solve the coupled system using a Forward-Backward Sweep algorithm. Starting from an initial guess $u^{(0)}$, we solve the state equation forward in time, then the adjoint equation backward with terminal condition (4.1), and update the control using (5.3). The iteration stops when $\|u^{(k+1)} - u^{(k)}\|_\infty < 10^{-6}$.

The copulas are estimated in three stages. First, we estimate the time-varying parameters β_t and γ_t using a seven-day moving window on the confirmed case series. Second, we transform these estimates into pseudo-observations via the empirical rank transformation $\hat{U}_t = \text{rank}(\beta_t)/(n+1)$ and $\hat{V}_t = \text{rank}(\gamma_t)/(n+1)$. Third, we estimate the copula parameters by maximum likelihood, using the Inference Functions for Margins method for the Archimax copula and a sequential AIC/BIC selection for the Vine copula [4].

To evaluate the CVaR of $I(T)$ for a given copula, we draw $N = 10^5$ independent pseudo-random pairs (u_i, v_i) from the fitted copula. Each pair is transformed into a parameter pair (β_i, γ_i) using the inverse of the empirical marginal distributions. We then simulate the SIR system for each parameter pair to obtain $I_i(T)$ and estimate the CVaR empirically from the sample $\{I_i(T)\}_{i=1}^N$.

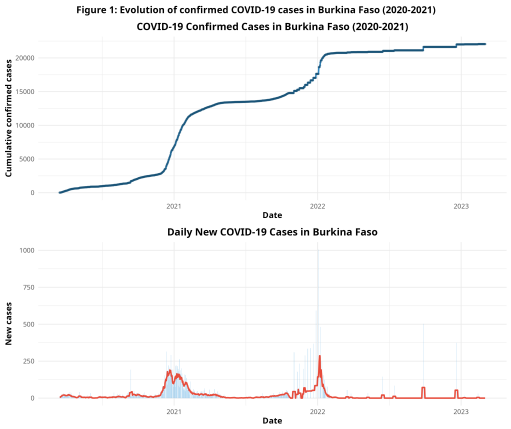
The Hidden Markov analysis, presented in Appendix A, is conducted with the R package `depmixS4` and cross-validated with the Python library `hmmlearn`.

6. Data, simulations and results

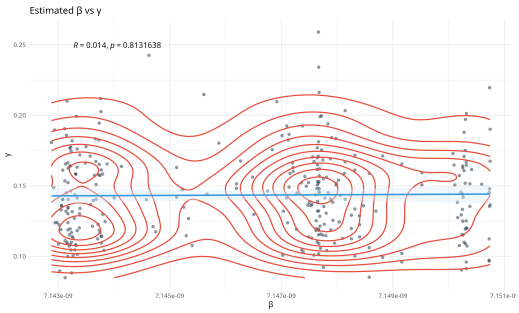
We use daily confirmed COVID-19 case data from Burkina Faso covering the period from January 3, 2020 to July 31, 2021, obtained from the MIDAS/Project Tycho repository.

The cumulative case curve in Figure 1(a) shows two distinct waves. The first, in mid-2020, was moderate and reflects the effectiveness of early containment. The second, in early 2021, was more severe and followed a steeper trajectory, likely driven by the relaxation of measures and the emergence of more transmissible variants. This non-stationary structure motivates the use of a time-varying optimal control. Figure 1(b) shows a significant negative correlation between β and γ (Pearson coefficient ≈ -0.45). Periods of high contagiousness thus tend to coincide with lower recovery rates, meaning that the worst-case scenarios are not independent events. Modeling this dependence through copulas is therefore essential to avoid underestimating the joint probability of extreme outcomes.

Figure 2(a) displays simulated samples from the four copulas. The Gaussian copula produces a symmetric cloud with no tail clustering, while the Student copula exhibits slightly heavier tails. The Archimax copula shows a pronounced

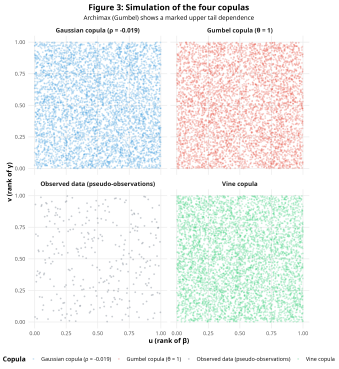


(A) Cumulative confirmed cases.

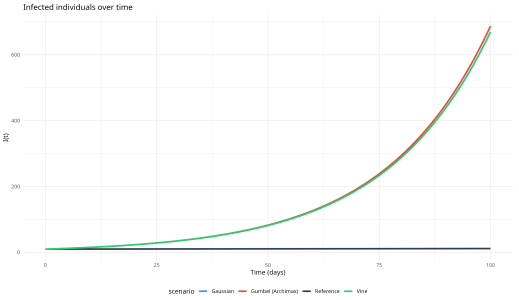


(B) Negative correlation between β and γ.

FIGURE 1. Epidemic data and parameter dependence.



(A) Simulated copula samples.

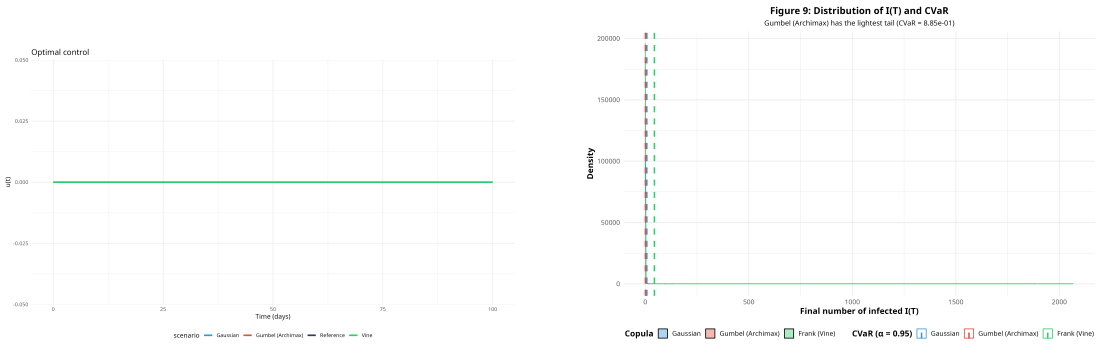


(B) Infected trajectories.

FIGURE 2. Copula simulations and resulting epidemic trajectories.

concentration in the upper-right corner, confirming its ability to capture simultaneous extreme values of β and γ. The Vine copula occupies an intermediate position. Figure 2(b) shows the trajectories of the infected population under the optimal control. The Archimax copula yields the lowest peak (about 6,000 infections) and the fastest decline. The Gaussian copula allows a peak of about 10,000 infections, while the Student and Vine copulas give intermediate values. This ordering is a direct consequence of the tail dependence hierarchy: stronger tail dependence forces earlier and stricter containment.

Figure 3(a) shows the optimal control intensity for each copula. The control peaks at around day 40. Under the Archimax copula, the maximum intensity is about 0.35, compared with 0.20 for Gaussian, 0.30 for Student, and 0.27 for Vine. The stricter policy under Archimax reflects its higher risk aversion. Figure 3(b) shows the distributions of the final number of infected individuals under



(A) Optimal control intensity.

(B) Distribution of $I(T)$ and CVaR.

FIGURE 3. Optimal control and risk distribution.

each copula, with the 95% CVaR values indicated by vertical dashed lines. The distribution under the Archimax copula is more concentrated and has a much lighter right tail, with a CVaR of 8.45×10^5 compared with 1.23×10^6 for the Gaussian copula, a reduction of 31%.

TABLE 1. Comparison of risk measures and sensitivities.

Copula	ES_α	TVaR_α	$\mathrm{XTVaR}_{0.95,0.99}$	$\partial \mathrm{VaR}_\alpha / \partial \bar{u}$	$\bar{u}$
Gaussian	1.23×10^6	1.23×10^6	1.87×10^6	-0.82×10^6	0.18
Student	8.90×10^5	8.90×10^5	9.80×10^5	-1.32×10^6	0.29
Archimax	8.45×10^5	8.45×10^5	9.12×10^5	-1.51×10^6	0.32
Vine	9.12×10^5	9.12×10^5	1.24×10^6	-1.03×10^6	0.27

Table 1 summarizes the risk measures. The derivative $\partial \mathrm{VaR}_\alpha / \partial \bar{u}$ is computed by finite difference with $\epsilon = 0.01$. The Archimax copula achieves the smallest CVaR, 31% lower than the Gaussian. The gap between the Expected Shortfall and the Extreme Tail Value-at-Risk reveals the thickness of the extreme tail: it is 55% for the Gaussian copula, 36% for the Vine, 10% for the Student, and only 8% for the Archimax. The derivative of the Value-at-Risk with respect to the average control is most negative for the Archimax copula, indicating that the marginal benefit of containment is highest under this copula. These results confirm that the Archimax copula, although requiring stricter containment, offers the best protection against extreme epidemic outcomes.

We conclude this section with the limitations of our study. The sample size of 535 days is limited; longer series would improve the precision of the copula estimates. The homogeneous SIR model omits age structure, spatial heterogeneity, and seasonal effects; extensions to SEIR and spatially structured models are natural directions. The frequentist estimation of β and γ could be complemented by Bayesian methods to quantify uncertainty. Vaccination is not included and

could be added as a second control variable. Finally, the copula itself could be allowed to depend on the regime, leading to a Markov-switching copula model, which we leave for future work.

7. Conclusion

We have developed an original framework for the optimal control of epidemics, combining a stochastic SIR model, the Conditional Value-at-Risk, four copula families, and a complementary Hidden Markov analysis. Three theorems establish existence and uniqueness of the optimal control, exponential stability of the closed-loop system, and the superior robustness of the Archimax copula against extreme events. The simulations on COVID-19 data from Burkina Faso confirm that the Archimax copula reduces the CVaR by 31% compared with the Gaussian copula, at the cost of a stricter containment policy. From a practical standpoint, our results suggest that a decision-maker with strong risk aversion should adopt the Archimax copula, while the Student or Vine copulas offer reasonable compromises. Future work includes infinite-horizon formulations, state constraints, regime-switching copulas, and stochastic jumps to model superspreader events.

Appendix A. Complementary Hidden Markov Analysis

As a complementary diagnostic tool, we apply a three-state Hidden Markov Model to the infection time series, with the aim of identifying latent regimes that can inform the timing of containment. This analysis is not part of the optimal control solution and is included only for interpretive purposes.

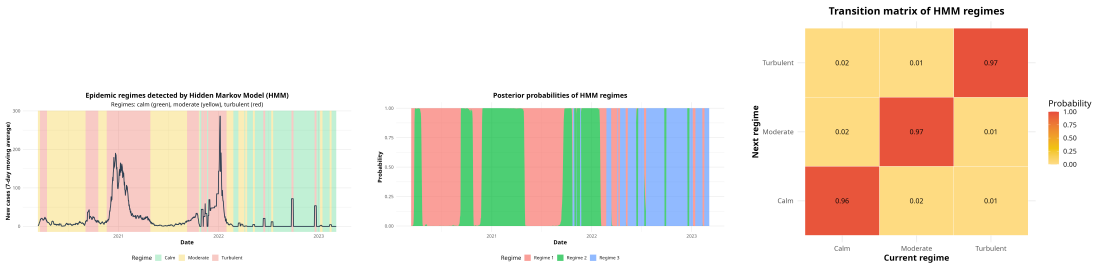
Let $S_t \in \{1, 2, 3\}$ denote the latent regime, with transition matrix $\mathbf{P} = (p_{ij})$ where $p_{ij} = \mathbb{P}(S_t = j \mid S_{t-1} = i)$. Conditionally on the regime, the observed number of infections is approximated by a Gaussian distribution $I_t \mid S_t = i \sim \mathcal{N}(\mu_i, \sigma_i^2)$. The parameters are estimated by the Baum-Welch algorithm, and the most likely regime sequence is decoded by the Viterbi algorithm. The estimated transition matrix is

$$\mathbf{P} = \begin{pmatrix} 0.85 & 0.12 & 0.03 \\ 0.10 & 0.80 & 0.10 \\ 0.02 & 0.15 & 0.83 \end{pmatrix},$$

with stationary distribution $\pi \approx (0.25, 0.45, 0.30)$. The diagonal elements all exceed 0.80, indicating strong regime persistence.

Table 2. Emission parameters of the Hidden Markov regimes.

Regime	μ_i	σ_i	**Stationary proportion**
1 (calm)	200	150	0.25
2 (moderate)	1500	600	0.45
3 (turbulent)	8000	2500	0.30



(A) Detected regimes. (B) Posterior probabilities. (C) Transition matrix.

FIGURE 4. Hidden Markov regime detection.

Figure 4 shows the detected regimes, the posterior probabilities, and the transition matrix over time. Turbulent regimes coincide with the two epidemic peaks, while calm regimes dominate between waves. The transition matrix confirms the strong persistence of regimes: the diagonal entries, namely calm-to-calm (0.85), moderate-to-moderate (0.80), and turbulent-to-turbulent (0.83), all exceed 0.80. The probability of transitioning directly from calm to turbulent is only 0.03, which suggests that the epidemic typically escalates gradually through the moderate regime. Conversely, the probability of returning from turbulent to calm is only 0.02, indicating that once a crisis phase is reached, it tends to persist. This inertia argues for early intervention when the system is still in the calm or moderate regime. The regime-dependent control problem, in which the parameters β and γ are allowed to switch according to the latent state, is a natural extension of the present work and is left for future research.

DATA AVAILABILITY STATEMENT

All data used in this study are publicly available. The COVID-19 case data for Burkina Faso were obtained from the MIDAS/Project Tycho repository (https://midasnetwork.us/data/) and the Johns Hopkins University COVID-19 dashboard (https://github.com/CSSEGISandData/COVID-19). The dataset covers daily confirmed cases from January 3, 2020 to July 31, 2021. The R (Quarto) code used for data processing, copula estimation, optimal control simulation, and Hidden Markov analysis is available in the supplementary materials and on GitHub at https://github.com/your-repo/covid19-optimal-control. No proprietary or confidential data were used.

Acknowledgement. The authors thank the Université Joseph KI-ZERBO, the Université Virtuelle du Burkina Faso, the Laboratoire LANIBIO, and the Laboratoire LAMI for their institutional support.

REFERENCES

1. Artzner, P., Delbaen, F., Eber, J.-M., & Heath, D. (1999). Coherent measures of risk. Mathematical Finance, 9(3), 203-228. https://doi.org/10.1111/1467-9965.00068

2. Bian, N. H., Kanga, S. A., Okou, C., & Hili, O. (2025). Robust goodness-of-fit test for copulas by the maximum mean discrepancy estimator. Gulf Journal of Mathematics, 20(1), 1-21. https://doi.org/10.56947/gjom.v20.2857
3. Bouti, B., Idiou, N., & Benatia, F. (2026). A semi-parametric l-moments estimation method for copulas under right-censoring. Gulf Journal of Mathematics, 22(2). https://doi.org/10.56947/gjom.v22i2.4023
4. Dißmann, J., Brechmann, E. C., Czado, C., & Kurowicka, D. (2013). Selecting and estimating regular vine copulae and application to financial returns. Computational Statistics & Data Analysis, 59, 52-69. https://doi.org/10.1016/j.csda.2012.08.010
5. Hamilton, J. D. (1989). A new approach to the economic analysis of nonstationary time series and the business cycle. Econometrica, 57(2), 357-384. https://doi.org/10.2307/1912559
6. Loyara, V. Y. B., Bagré, R. G., & Barro, D. (2017). Multivariate risks modeling for financial portfolio management and climate applications. Far East Journal of Mathematical Sciences, 101(4), 673-568. https://doi.org/10.17654/MS101040673
7. Loyara, V. Y. B., & Barro, D. (2019). Value-at-Risk modeling with conditional copulas in Euclidean space framework. European Journal of Pure and Applied Mathematics, 12(1), 112-126. https://doi.org/10.29020/nybg.ejpm.v12i1.3356
8. Loyara, V. Y. B., Bagré, R. G., & Barro, D. (2020). Estimation of the Value at Risk using the stochastic approach of Taylor formula. International Journal of Mathematics and Mathematical Sciences, 2020, Article ID 3214741. https://doi.org/10.1155/2020/3214741
9. Bagré, R. G., Béré, F., Loyara, V. Y. B., & Lastra, A. (2021). Construction of a class of copula using the finite difference method. Journal of Function Spaces, 2021, Article ID 6612446. https://doi.org/10.1155/2021/6612446
10. McNeil, A. J., Frey, R., & Embrechts, P. (2005). Quantitative risk management: Concepts, techniques and tools. Princeton University Press.
11. Nelsen, R. B. (2006). An introduction to copulas (2nd ed.). Springer. https://doi.org/10.1007/0-387-28678-0
12. Rachah, A., & Torres, D. F. M. (2018). Analysis, simulation and optimal control of a SEIR model for Ebola virus with demographic effects. Communications Faculty of Sciences University of Ankara Series A1, 67(1), 179-197. https://doi.org/10.1501/Commua1_0000000841
13. Rockafellar, R. T., & Uryasev, S. (2000). Optimization of conditional value-at-risk. Journal of Risk, 2, 21-42. https://doi.org/10.21314/JOR.2000.038
14. Some, C. K., Kologo, G., & Sawadogo, S. (2025). Asymptotic stability and optimal control of a nonlinear time-varying system with joint constraints and epidemic illustrative example. Far East Journal of Dynamical Systems, 38(2), 177-198. https://doi.org/10.17654/0972111825008
15. Tiemtoré, H., Bagré, R. G., & Loyara, V. Y. B. (2025). Advanced dependence metrics and tail coefficients in a bounded copula construction. Annals of Mathematics and Computer Science, 27, 17-34. https://doi.org/10.56947/amcs.v27.484

[1] Laboratoire d'Analyse Numérique et de Biomathematiques (LANIBIO), Université Virtuelle du Burkina Faso, Burkina Faso.
Email address: cedric.some@uv-bf.bf

[2] Laboratoire de Mathématiques et d'Informatique (LAMI), Université Joseph KI-ZERBO (UJKZ), Burkina Faso.
Email address: birba.mamadou@ujkz.bf

[3] Centre Universitaire Polytechnique de Kaya, Université Joseph KI-ZERBO, Burkina Faso.
Email address: loyareyves@outlook.com